PROJECTION OF ANNUAL CROP COEFFICIENTS IN ITALY BASED ON CLIMATE MODELS AND LAND COVER DATA

Mărgărit-Mircea NISTOR[1*]

DOI: 10.21163/GT_2018.132.08

ABSTRACT:
Nowadays, a multitude of world changes are coming to affect the ecosystems, urban landscapes, and natural resources. Land use and land cover patterns represent an interactive layer between Earth surface and underground entities which is often consider in the hydrogeological studies. Many factors such as climate parameters and human activities affects the groundwater recharge, quality of water resources and also changes in the hydrologic regime. Crop evapotranspiration plays an essential role in the water balance and water deficit investigations. Here, we use the seasonal crop coefficients to calibrate the annual crop coefficients for the Italian territory. These values could be useful for the temperate zone area. Four stages of annual crop coefficients were set (initial, mid-season, end season, cold season) to perform the calculation of annual crop coefficients. The annual crop coefficients (AKc) have been extracted from the annual ETc. CORINE land cover data and high resolution climate models of potential evapotranspiration (ET0) were the key datasets for AKc projection in Italy. These findings and original maps that we show in the paper represent important tools for the agriculture, environmental, and urban planning.

Keywords: land cover, seasons, crop coefficients, crop evapotranspiration, land cover projections, Italy.

1. INTRODUCTION

In several cases, the climate change have had negative impact on surface water resources and groundwater (Loàiciga et al., 2000; Parmesan & Yohe, 2003; Brouyère et al., 2004; Campos et al., 2013; Prăvălie et al., 2014). It was shown that the ecosystems and it's ecolines are very sensitive to climate change, biodiversity and composition can have consistent changes. In addition to climate change, the land cover and land use pattern play an important role in the interface of land and atmosphere.

Slightly changes of land cover may disturb the entire functions of the ecosystems, which preserve the equilibrium in various domain: e.g. effect on water vulnerability in the regional and local hydrology, cultivation patterns in agriculture, and the evapotranspiration regime as a climatic parameter.

[1] *Nanyang Technological University, School of Civil and Environmental Engineering, 639798, Singapore; margarit@ntu.edu.sg*

Both climate and land cover are direct responsible for the evapotranspiration phenomena, fact for which many hydrological studies used the potential evapotranspiration and actual evapotranspiration for water balance and water surplus investigations (Li et al., 2007; Rosenberry et al., 2007; Gowda et al., 2008). The land cover changes on short-term could be detected by satellite images (Angelini et al., 2017), which are now available at high resolution. In the last years, Adamo et al. (2014) predicted the shoreline changes using the coastal erosion model based on altimeters and directional wave spectrum. Rogana & Chen (2004) have applied the remote sensing to identify and monitor the land cover and land use changes. In their study, the techniques of data collection from sensors, spatial resolution and data processing were discussed. Moreover, geographic information systems (GIS) and image analysis systems, become together strong tools in the land cover changes mapping (Treitz & Rogan, 2004). However, in this study, we have focused on CORINE Land Cover and Hercules models, because these databases are already validated and available for scientists' community.

A substantial contribution was the FAO Paper no. 56 (Allen et al., 1998) and Allen's work (Allen, 2000) that proposed a complex methodology to calculate the crop evapotranspiration (ET_c) and to carry out the K_c/evapotranspiration rate for different type of crops. In the same years, Grimmond & Oke (1999) done the measurements of evapotranspiration in various cities from United States and further they calculated the K_c related not only for crops and plants, but also for urban areas and impervious fractions. Integrating the K_c in the formula of ET_c, Nistor et al. (2017) calculated the ET_c for regional scale in four seasons for the Pannonian basin. They extracted the K_c from the CORINE Land Cover database and, considering the growth of crops period they divided the year months in the crop calendar. Thus, initial, mid-seasons, end season and cold seasons were the main periods for which they have calculated the seasonal ET_c. Summing the values of seasonal ET_c, the total annual ET_c was found.

The aim or our work was to complete the spatial distribution of seasonal K_c related to four stages of crop calendar and to calculate the annual K_c for the Italian territory. We choose this land because is composed by a heterogeneous landscape including almost all relief types and extends on more than 10 degrees in latitude, which implies an advantage for the annual K_c calculation in temperate zone. Moreover, Italian territory has a large coastal zone, with a diversity of vegetation cover, but also and the climate is complex in Italy. The findings carried out through our methodology are a huge contribution for climatologist and hydrogeologists due to a final product map annual K_c for present and future.

2. STUDY AREA

Italian territory extends from 36°38' to 47°4' North and 6°38' to 18°32' East (GCS_WGS_1984 Projection) and is located in south of Europe (**Fig. 1**). Italy is a Mediterranean country, with a large coastal lines, various orography and complex climate. Thus, the eastern coast is bordered by Adriatic sea from North to South, the South and southeastern sides of the country are mainly bordered by Ionian Sea and Mediterranean Sea, when the northwestern and western sides of Italy are bordered by Ligurian Sea respective Tyrrhenian Sea. Attached to Italy are also Sicily and Sardinia Islands, but also many small islands.

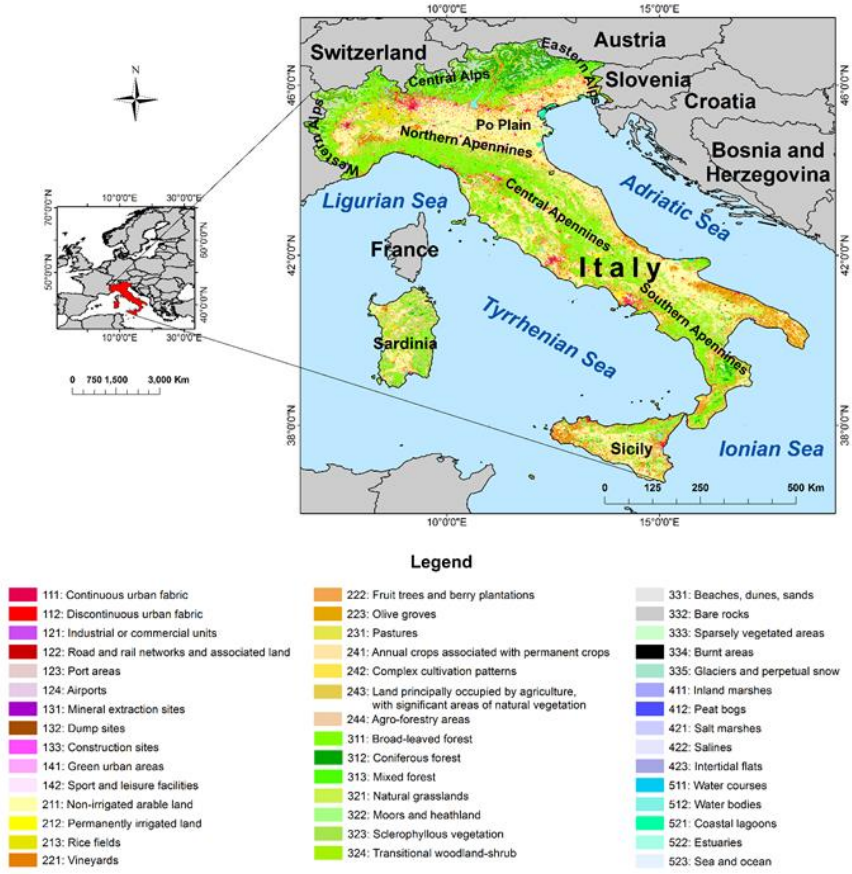

Fig. 1. Location of the Italy on the Europe map (left) and land cover of the Italian territory (right).

Regarding the relief of the Italy, the major mountain belts are the Alps Mountains in North (Western Alps, Central Alps, and Eastern Alps) and Apennines Mountains (Northern Apennines, Central Apennines, and Southern Apennines) that extends from northwestern to southeastern through the central part of the Italian Peninsula. The main lowlands are Po Plain and Po River Delta, located in North sides of the country, but also the Adriatic coast represents the realm with lows elevations.

From climate point of view, the Cfa and Cfb are the main climate in the North of the country (Kottek et al., 2006) with Csa climate in the South. The mean annual temperature for the actual period in the study area ranged from -0.5 °C in North to 18.4 °C in South. The mean annual precipitation in the present period exceeds 1800 mm year^{-1} in many locations of Alps and Northern Apennines and the maximum values reach 2100 mm year^{-1} in the Northern Apennines. The ET_0 in Italy ranged from 367 mm up to 927 mm. The maximum values of ET_c (1299 mm) are found in the South of the Italy, but also the values over 1200

mm of ET_c are found in Sicily and West side of Sardinia. The highest value of ET_c in that area is influenced by the high temperatures and high K_c of vegetation (e.g. broad-leaved forest). The adapted vegetation at orography and climate were identified in Italy. In mountains areas the main covers are coniferous and mixed forest which included species as oak (Quercus), beech (Fagus), elms (Ulmus), and hornbeam (Carpinus) (European Environment Agency, 2007), pasture and transnational woodland and shrubs. The lowlands and plains are mainly covered by hay, herbaceous vegetation and agricultural lands. In the hilly areas and in the meadows along rivers are presents more broad-leaved forests and shrubs. The coastal areas are predominantly with Mediterranean vegetation as Italian stone pine (Pinus pinea), green areas, and sclerophyllous vegetation. On the coast zone are also located the ports areas, the lagoons and marshes.

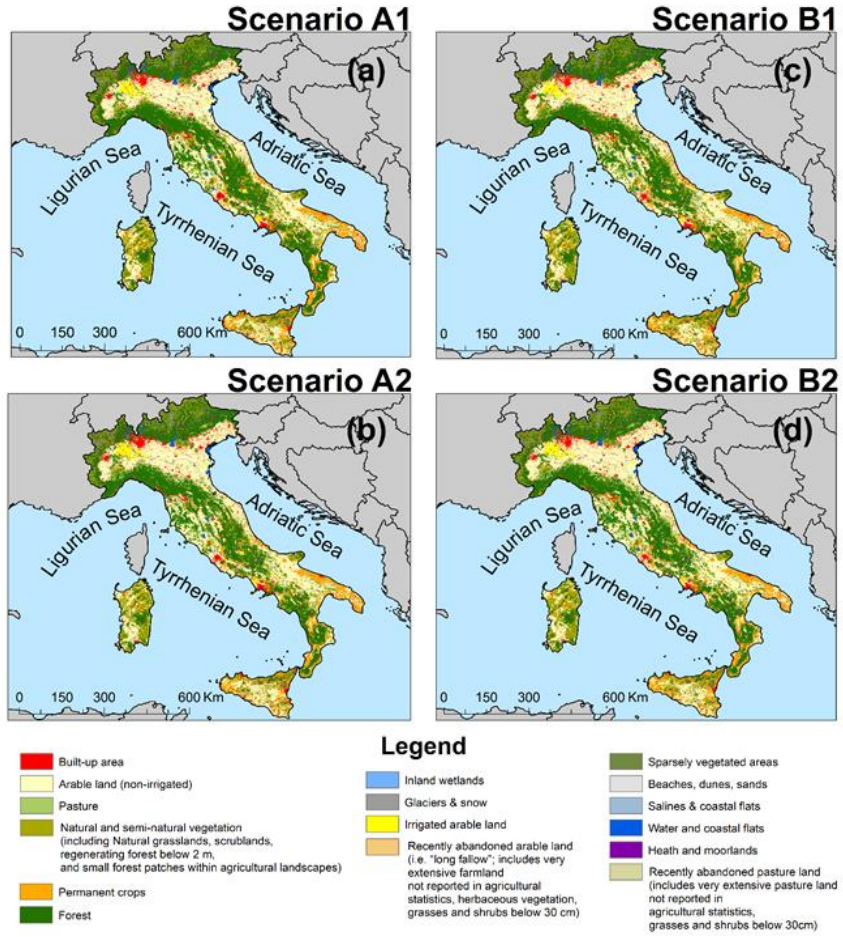

Fig. 2. Land cover projections of Italy. (a) Scenario A1. (b) Scenario A2. (c) Scenario B1. (d) Scenario B2. Source: Sustainable futures for Europe's HERitage in CULtural landscapES" project (http://www.hercules-landscapes.eu/).

3. MATERIALS AND METHODS

3.1. CORINE land cover data

Raster data with 250 m spatial resolution of CORINE Land Cover 2012 served to identify represent the land type categories in Italy for the present period. This database was elaborated by Copernicus Land Monitoring Services (2012) and cover the northern, southern, western and central sides of Europe.

Dynamic spatial changes of the land use and land cover for the future period have been depicted using the Hercules models carried out in the "Sustainable futures for Europe's HERitage in CULtural landscapES" project, GA no. 603447 (Schulp et al., 2015). Using four scenarios, Schulp et al. (2015) projected the land cover of Europe by 2040 based on macro-economic and land use models for which they set fourteen trajectories in the land trend considering the urbanization, agriculture and forestry.

The raster data of future Hercules models are available on website (http://www.hercules-landscapes.eu/) while the procedure of the trajectories, indices and mapping cultural landscapes is highlighted in the Report no. 1 off the Hercules project (Schulp et al., 2015). Four scenarios as A1, A2, B1, and B2 in sixteen classes (**Fig. 2**) built for 2040 were used for the present paper to represent the spatial distribution of seasonal K_c.

3.2. Seasonal crop coefficients (Kc)

According to Allen et al. (1998) and Grimmond & Oke (1999), for each land cover type was assigned a certain crop coefficient (K_c) value. Based on these values, the ET_c calculation for four season and annual periods were done.

Allen et al. (1998) have mentioned tested values and a detailed analyzed K_c for various climate zones (e.g. Tropics, Temperate, and Mediterranean) in the Food and Agriculture Organization report. The K_c related to the urban areas and bare soil have been calculated and published by Grimmond & Oke (1999). Four stages of crop growth and specified K_c for have been considered in this study, as follow: initial season ($K_{c\ ini}$) during the March, April, May; mid-season ($K_{c\ mid}$) during June, July, August; end season ($K_{c\ end}$) during September and October; cold season ($K_{c\ cold}$) during January, February, November, and December. Here, we adopt the Nistor et al. (2017) methodology to illustrate the spatial distribution of K_c in Italy and to carry out the annual crop coefficients (AK_c). At regional scale, due to the overlap of growth crops calendar, the scientists insert this stage in the initial season (Nistor et al., 2017). The standard K_c values for initial season, mid-season, end season, and cold season related to the present and future are reported in the Table 1, respective Table 2.

Table 1. Corine Land Cover classes and representative seasonal Kc coefficients for the present in Italian territory

Corine Land Cover		Kc ini season	Kc mid season	Kc end season	Kc cold season
CLC code 2012	CLC Description	Kclc	Kclc	Kclc	Kclc
111	Continous urban fabric	0.2	0.4	0.25	-
112	Discontinuous urban fabric	0.1	0.3	0.2	-
121	Industrial or commercial units	0.2	0.4	0.3	-
122	Road and rail networks and associated land	0.15	0.35	0.25	-
123	Port areas	0.3	0.5	0.4	-
124	Airports	0.2	0.4	0.3	-
131	Mineral extraction sites	0.16	0.36	0.26	-
132	Dump sites	0.16	0.36	0.26	-
133	Construction sites	0.16	0.36	0.26	-
141	Green urban areas	0.12	0.32	0.22	-
142	Sport and leisure facilities	0.1	0.3	0.2	-
211	Non-irrigated arable land	1.1	1.35	1.25	-
212	Permanently irrigated land	1.2	1.45	1.35	-
213	Rice fields	1.05	1.2	0.6	-
221	Vineyards	0.3	0.7	0.45	-
222	Fruit trees and berry plantations	0.3	1.05	0.5	-
223	Olive groves	0.65	0.7	0.65	0.5
231	Pastures	0.4	0.9	0.8	-
241	Annual crops associated with permanent crops	0.5	0.8	0.7	-
242	Complex cultivation patterns	1.1	1.35	1.25	-
243	Land principally occupied by agriculture, with significant areas of natural vegetation	0.7	1.15	1	-
244	Agro-forestry areas	0.9	1.1	1.05	0.3
311	Broad-leaved forest	1.3	1.6	1.5	0.6
312	Coniferous forest	1	1	1	1
313	Mixed forest	1.2	1.5	1.3	0.8
321	Natural grasslands	0.3	1.15	1.1	-
322	Moors and heathland	0.8	1	0.95	-
323	Sclerophyllous vegetation	0.25	0.9	0.8	-
324	Transitional woodland-shrub	0.8	1	0.95	-
331	Beaches, dunes, sands	0.2	0.3	0.25	-
332	Bare rocks	0.15	0.2	0.05	-
333	Sparsely vegetated areas	0.4	0.6	0.5	-
334	Burnt area	0.1	0.15	0.05	-
335	Glaciers and perpetual snow	0.48	0.52	0.52	0.48
411	Inland marshes	0.15	0.45	0.8	-
412	Peat bogs	0.1	0.4	0.75	-
421	Salt marshes	0.1	0.3	0.7	-
422	Salines	0.1	0.15	0.05	-
423	Intertidal flats	0.3	0.7	1.3	-
511	Water courses	0.25	0.65	1.25	-
512	Water bodies	0.25	0.65	1.25	-
521	Coastal lagoons	0.3	0.7	1.3	-
522	Estuaries	0.25	0.65	1.25	-
523	Sea and ocean	0.4	0.8	1.4	-

Kc - crop coefficient for plants, Ks - evaporation coefficient for bare soils, Ku - crop coefficient for urban areas, Kw - evaporation coefficient for open water, Kclc - crop coefficient for land cover. Source: From Allen et al. (1998); Nistor et al. (2017)

Table 2. Corine Land Cover classes and representative seasonal Kc coefficients used for the future scenarios in Italian territory

Corine Land Cover			Kc ini season	Kc mid season	Kc end season	Kc cold season
CLC code 2012	CLC projection code	CLC Description	Kclc	Kclc	Kclc	Kclc
133	0	Built-up area	0.16	0.36	0.26	-
211	1	Arable land (non-irrigated)	1.1	1.35	1.25	-
231	2	Pasture	0.4	0.9	0.8	-
321 and 324	3	Natural and semi-natural vegetation (including Natural grasslands, scrublands, regenerating forest below 2 m, and small forest patches within agricultural landscapes)	0.45	1.1	1	-
411	4	Inland wetlands	0.15	0.45	0.8	-
335	5	Glaciers and snow	0.48	0.52	0.52	0.48
212	6	Irrigated arable land	1.2	1.45	1.35	-
321	7	Recently abandoned arable land (i.e. "long fallow"; includes very extensive farmland not reported in agricultural statistics, herbaceous vegetation, grasses and shrubs below 30 cm)	0.3	1.15	1.1	-
241	8	Permanent crops	0.5	0.8	0.7	-
313	10	Forest	1.2	1.5	1.3	0.8
333	11	Sparsely vegetated areas	0.4	0.6	0.5	-
331	12	Beaches, dunes and sands	0.2	0.3	0.25	-
422	13	Salines	0.1	0.15	0.05	-
423 and 521	14	Water and coastal flats	0.3	0.7	1.3	-
322	15	Heathland and moorlands	0.8	1	0.95	-
231 and 324	16	Recently abandoned pasture land (includes very extensive pasture land not reported in agricultural statistics, grasses and shrubs below 30cm)	0.6	1	0.9	-

Kc - crop coefficient for plants, Ks - evaporation coefficient for bare soils, Ku - crop coefficient for urban areas, Kw - evaporation coefficient for open water, Kclc - crop coefficient for land cover. Source: From Allen et al. (1998); Nistor et al. (2017)

3.3.Climate data

Mean monthly air temperature models related to 2011 to 2040 served to carried out the seasonal ET_0 in the present study and to calculate the seasonal and annual ET_c. The climate models are in raster grid format at very high spatial resolution with a temporal average of 30 years. Based on the ANUSplin software, Hamann et al. (2013) have completed the air temperature models for Europe. These models are courtesy by Andreas Hamann from Alberta University, Canada. The climate models were generated using the ClimateEU v4.63 software package (see http://tinyurl.com/ClimateEU) and followed the methodology described by Hamann et al. (2013).

3.4. Annual crop evapotranspiration (ET_c) and annual crop coefficient (AK_c)

The AK_c is the ratio expression of ET_c and ET_0. Based on the seasonal values of K_c and climate data, the seasonal and annual ET_c have been calculated. Firstly, for the each set season was performed the ET_0 using the Thornthwaite (1948) method (Eq. 1). By multiplying the ET_0 of season K_c, the ET_c related to the four seasons were calculated (Eqs. 4-7). The annual ET_c is the sum of initial ET_c, mid-season ET_c, end season ET_c and cold season ET_c (Eq. 8). Divided the annual ET_c at the ET_0, the AK_c (Eq. 9) was found for the present and further, implemented for the future scenarios. Further, from the annual ET_c and ET_0, the average value of AK_c for each land cover type was extracted. Using the pinpoint verification on the Italian map, the specific value of the AK_c were assigned to the respective land cover type.

$$ET_0 = 16(\frac{10T_i}{I})^{\alpha} \quad (1)$$

$$I = \sum_{i=1}^{12} \left(\frac{T_i}{5}\right)^{1.514} \quad (2)$$

where:

ET_0 monthly potential evapotranspiration [mm]

T_i average monthly temperature [°C], ET_0=0 if $\bar{Tm}$ <0

I heat index (Eq.(2))

α complex function of heat index (Eq. (3))

$$\alpha = 6.75 \times 10^{-7} I^3 - 7.71 \times 10^{-5} I^2 + 1.7912 \times 10^{-2} I + 0.49239 \quad (3)$$

where:

I annual heat index

$$ET_{c\ ini} = ET_{0\ ini} \times K_{c\ ini} \quad (4)$$

$$ET_{c\ mid} = ET_{0\ mid} \times K_{c\ mid} \quad (5)$$

$$ET_{c\ end} = ET_{0\ end} \times K_{c\ end} \quad (6)$$

$$ET_{c\ cold} = ET_{0\ cold} \times K_{c\ cold} \quad (7)$$

$$Annual\ ET_c = ET_{c\ ini} + ET_{c\ mid} + ET_{c\ late} + ET_{c\ cold} \quad (8)$$

$$AKc = \frac{ETc\ annual}{ET0\ annual} \quad (9)$$

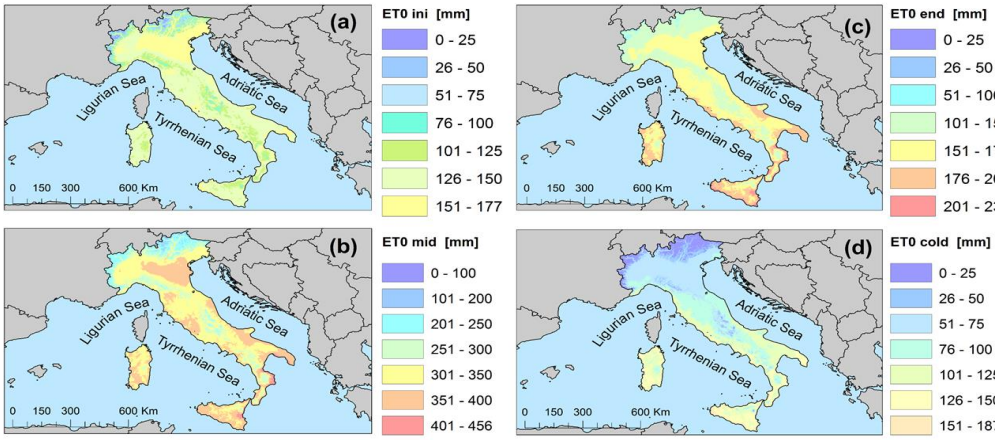

Fig. 3. Spatial distribution of seasonal ET_0 in Italy. (a) $ET_{0\ ini}$ for the initial season. (b) $ET_{0\ mid}$ for the mid-season. (c) $ET_{0\ end}$ for the end season. (d) $ET_{0\ cold}$ for the cold season.

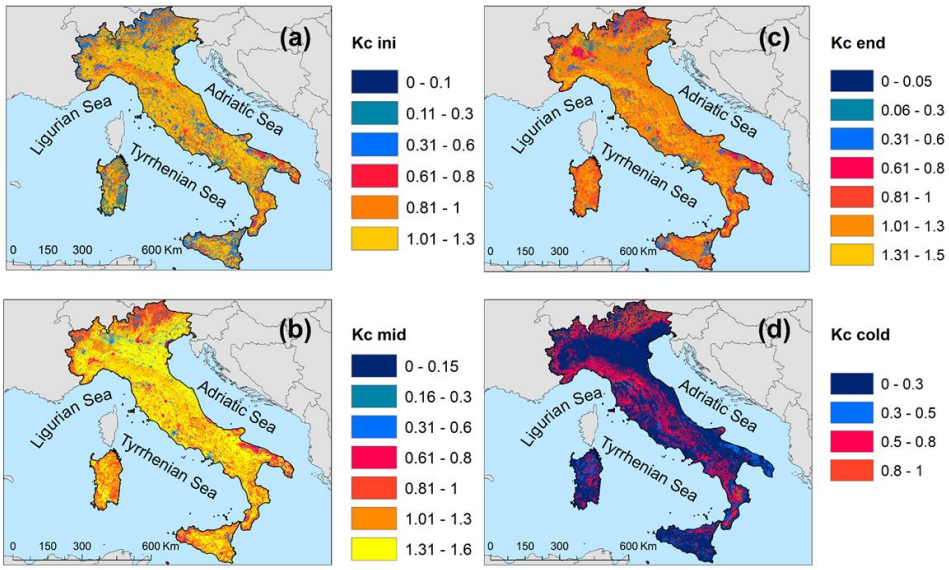

Fig. 4. Spatial distribution of K_c in Italy related to the present land cover. (a) $K_{c\ ini}$ for the initial season. (b) $K_{c\ mid}$ for the mid-season season. (c) $K_{c\ end}$ for the end season. (d) $K_{c\ cold}$ for the cold season.

4. RESULTS

Figure 3 depicts the seasonal ET_0 in Italy, carried out from the monthly ET_0. For the initial season, the ET_0 varies from 0 to 177 mm, the maximum values were found in the Po Plain and southeastern sides of Italy, on the coastal area. The mid-season ET_0 ranges from 0 to 456 mm, with the several places where the values exceed 300 mm. These sides overlap to Po Plain, coastal areas, central sides of the country and to the Sicily and Sardinia Islands. The values of the ET_0 in the end season varies from 0 to 230 mm, the southern parts and the islands are the main land with the high ET_0. As we expected, the cold season illustrates lower values of ET_0, especially in the North of Italy. In the Central Apennines, northern plains, and in the Alps regions the ET_0 fall below 75 mm. In the South, South-East, and South-West, but also in the Sicily and Sardinia Islands, the ET_0 register values above 100 mm in the cold season. In aim to calibrate the AK_c for the Italian territory, an detailed analysis of the K_c spatial distribution were done. Thus, the $K_{c\ ini}$ varies in the present period from 0 to 1.3 showing a large part of Italy with high coefficient. In the northern sides, excepting the Alps area and cities, the K_c register values above 1. The same trend is also on the Tyrrhenian and Adriatic coast, while in the South of Italy the values are around 0.81 – 1 in most of the territory, and fall below 0.6 in South of Sardinia, West and East of Sicily. The $K_{c\ mid}$ ranges from 0 to 1.6 and indicates high values in the Po Plain, northern and eastern coast, in central and south-central Italy, and on western coast. The southeastern, southern and northern parts of Italy shows values between 0.61 and 1. The most part of Sicily and Sardinia are covered by lands with values of 0.61 to 1.3 for $K_{c\ mid}$, but there are

also values which exceed 1.3. In the end season the $K_{c\ end}$ varies from 0 to 1.5 and the major part of territory has values between 0.81 and 1.3. The North of Italy, especially in the Alps Mountains, but also around the big cities, southeastern sides of country, West and East of Sicily the $K_{c\ end}$ fall below 0.6. During the cold season, 0.3 and less values are predominantly in the Italian land. In this season, opposite to the others, the Alps, Northern Apennines, and Central Apennines, and elevated parts of Sicily and Sardinia indicates highest values of the $K_{c\ cold}$ due to the presence of the forest cover, which has the high evapotranspiration rate also in the cold seasons. **Figure 4** illustrates the K_c spatial distribution in Italy during the four seasons related to the present period.

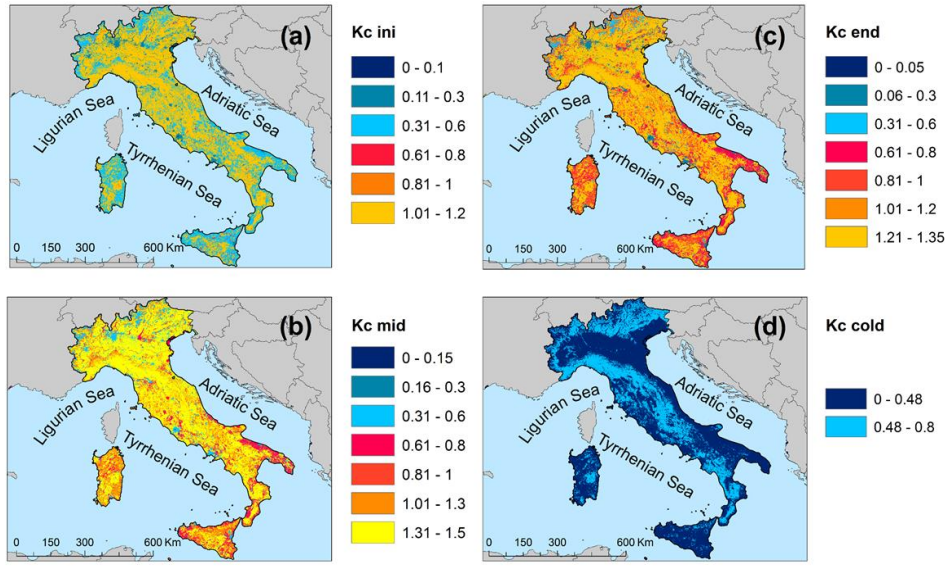

Fig. 5. Spatial distribution of K_c in Italy related to the projection of scenario A1. (a) $K_{c\ ini}$ for the initial season. (b) $K_{c\ mid}$ for the mid-season season. (c) $K_{c\ end}$ for the end season. (d) $K_{c\ cold}$ for the cold season.

The future projection of the land cover indicates slightly differences of the K_c pattern for all seasons due to the simplified land cover classes carried out for 2040. The $K_{c\ ini}$ varies in the future from 0 to 1.2 with values between 1 and 1.2 in the northern and inside central peninsula sides, while on the coastal areas, major land of Sicily and Sardinia, and Alps Mountains the values of $K_{c\ ini}$ ranges from 0.11 to 0.6. The K_c in the mid-season increase up to 1.5 and shows large parts of Italian territory with $K_{c\ mid}$ values over 1.3. These values extends in the North of the country, central and South of the Italian Peninsula. Southeastern and some southern sides of Italy, western, northern, and eastern parts of Sicily, central and North of Sardinia has medium values of $K_{c\ mid}$ (0.6 to 1). The Kc end varies for the future scenarios from 0 to 1.35, with elevated values (1 to 1.35) in the central and northern areas of Italy, while the southern areas of Italy, Sicily and Sardinia are cover more by land with Kc end values between 0.6 and 1.

The lowest values are located in the elevated mountains and surrounding the large urban areas and in the metropolitan area of the capital. In the cold season, the $K_{c\ cold}$ illustrates the lowest values of evapotranspiration rate and, more than this, only values below 1.

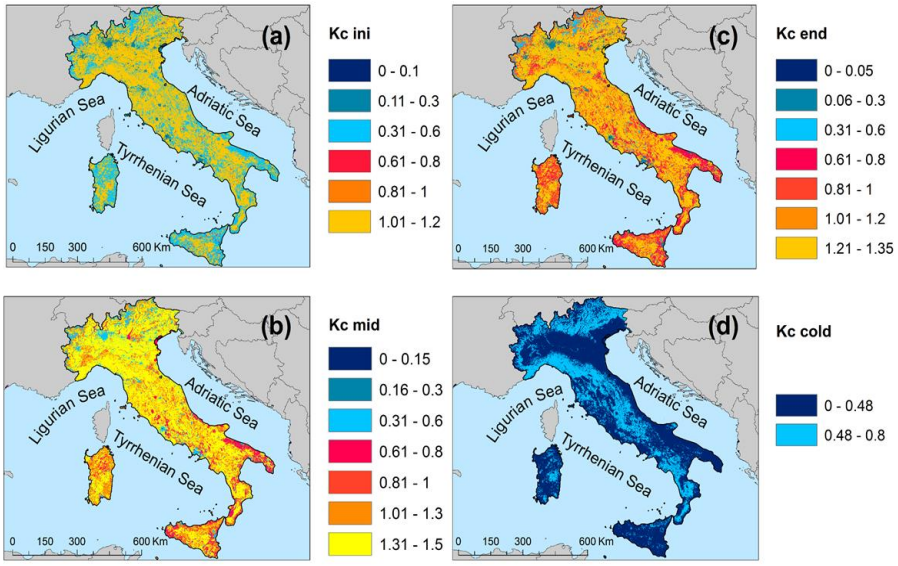

Fig. 6. Spatial distribution of K_c in Italy related to the projection of scenario A2. (a) $K_{c\ ini}$ for the initial season. (b) $K_{c\ mid}$ for the mid-season season. (c) $K_{c\ end}$ for the end season. (d) $K_{c\ cold}$ for the cold season.

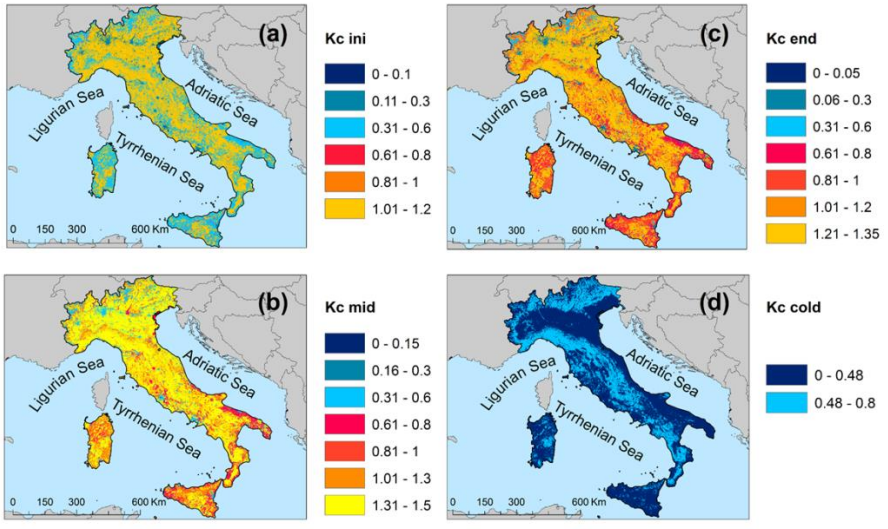

Fig. 7. Spatial distribution of K_c in Italy related to the projection of scenario B1. (a) $K_{c\ ini}$ for the initial season. (b) $K_{c\ mid}$ for the mid-season season. (c) $K_{c\ end}$ for the end season.

(d) $K_{c\ cold}$ for the cold season.

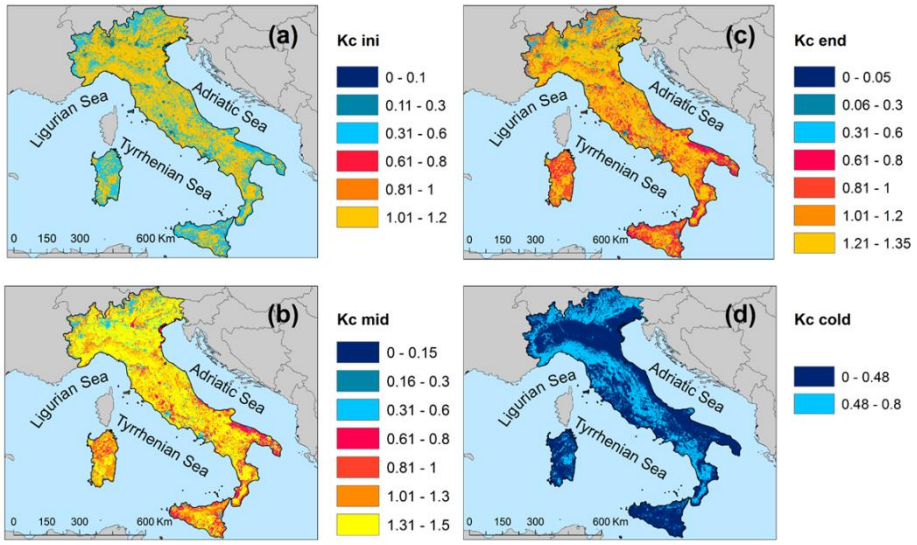

Fig. 8. Spatial distribution of K_c in Italy related to the projection of scenario B2. (a) $K_{c\ ini}$ for the initial season. (b) $K_{c\ mid}$ for the mid-season season. (c) $K_{c\ end}$ for the end season. d) $K_{c\ cold}$ for the cold season.

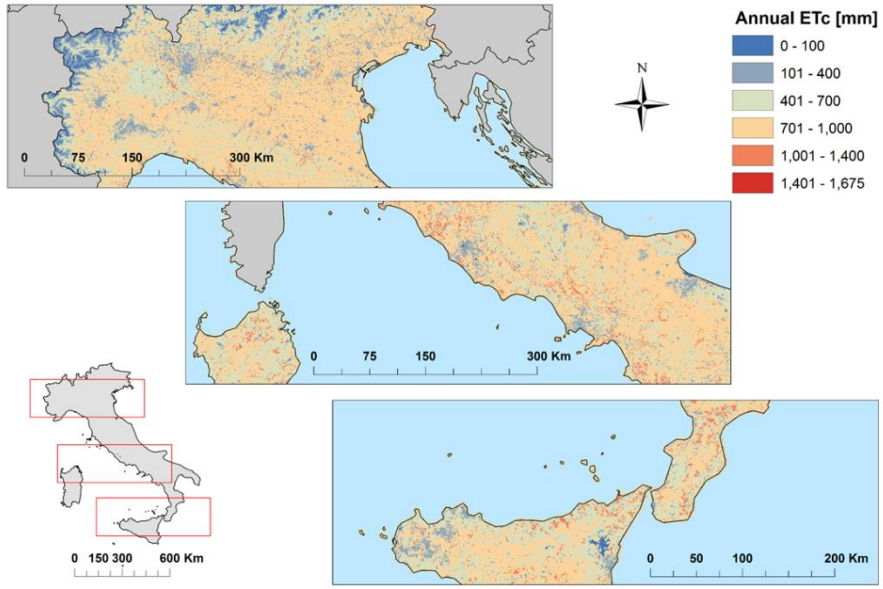

Fig. 9. Spatial distribution of annual ET_c in Italy related to the present (details of three sides).

Thus, in the mountain areas covered by forest and trees, the $K_{c\ cold}$ varies from 0.48 to 0.8, while in the plains, coastal areas, urban areas, Sicily and almost whole territory of Sardinia the values are 0. The pattern of $K_{c\ ini}$, $K_{c\ mid}$, $K_{c\ end}$, and $K_{c\ cold}$, are very similar for all scenarios. **Figures 5 – 8** show the variation of K_c in the Italian land considering the four seasons. Following the presented methodology, from the seasonal ET_0 and seasonal K_c, the annual ET_c was calculated for the present in aim to extract the AK_c. **Figure 9** illustrates three sheets of Italian Peninsula where the annual ET_c is more diversified and the values pattern can be observed in details.

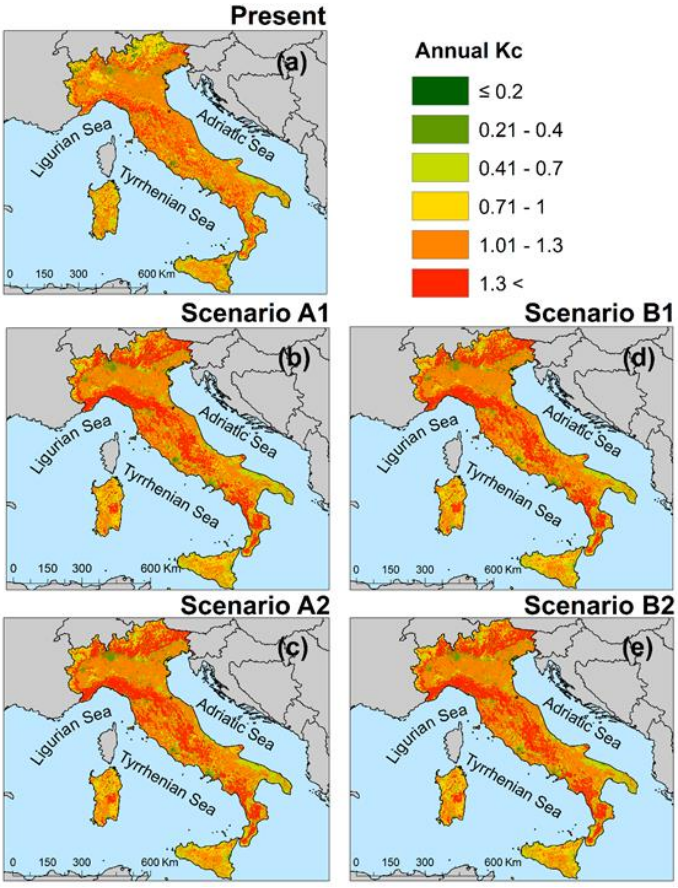

Fig. 10. Spatial distribution of AK_c in Italy related to the present and future projection. (a) AK_c for the present. (b) AK_c for the Scenario A1. (c) AK_c for scenario A2. (d) AK_c for the scenario B1. (e) AK_c for the scenario B2.

The annual ET_c ranges from 0 to 1675 mm, indicating the lowest values (below 400 mm) in the mountain areas, in the urban and in the no vegetated areas. The high values of annual ET_c were depicted in the all three set sheets, especially in many sides of the North,

central and South of Italy, where the ferest area is located. After the ratio of ET_c and ET_0, the AK_c have been calculated for Italy using the present climate and land cover layers.

Figure 10 depicts the AK_c spatial distribution for the present and future. Few territories has low values of AK_c (below 0.2) and are located in the North of Italy, some sides of Tyrrhenian coast, and in the agglomerated urban areas. The highest values (above 1.3) of the AK_c could be found in the Alps and Apennines Ranges while in the plains, and coastal areas the values of AK_c varies from 1 to 1.3. The southeastern part of Italy, western and eastern parts of Sicily, the AK_c has values between 0.4 and 0.7. Table 3 reports the calibrated values of AK_c for the present and Table 4 reports the AK_c for the future.

5. DISCUSSION AND CONCLUSIONS

Spatial distribution of seasonal K_c in Italy have been mapped for the present and future period. From the annual ET_c calculation, the AK_c specified for all classes of land cover was found. Due to the detailed division of CORINE Land Cover up to 4th level, the present AK_c map illustrates a distribution of crops presence mare diversified than in the future scenarios. In all cases, the high values of AK_c extends in the North of Italy, more precise in Prealps areas between Po Plain and Alps, in the Northern and Central Apennines, where the forest and the crops with evapotranspiration capacity rate rise over 1.3, but also in some sides of the South of Italy, Sicily and Sardinia. The lower AK_c (below 0.4) were depicted din the high mountains areas and surrounding the big cities.

Under the land cover projections, the land with high values of AK_c extends up to 2040, the scenario A1 is the most alarming for the Italian territory. Is the evolution of land cover will follow this scenario, the direct negative effects on agriculture and water resources will affected due to the irrigation water quantity requires.

Our work has obvious some limitations, not really from the calculation survey but more related to some aspects of missing field measurements. The complex land of Italy and the spatial extension no not allow us to complete an exhaustive study by tensiometers and lysimeters. For the same reason, in the Thornthwaite equation, the latitude factor of sunshine was set at 1. These limitations doesn't affects the investigations considering the large scale of the study, but also the appropriate results carried out here are in range with other studies about K_c and ET_c in central and southern Europe.

Present and future maps of seasonal K_c and AK_c at spatial scale of Italy represent significant tools for climatologists and hydrogeologists from one of the larger and complex country from Europe. Based on these maps, the water deficit and water surplus for different locations of the country may be calculated.

Acknowledgements

The authors would like to thank to the Copernicus Land Monitoring Services, which provided the land cover data for the present study. Many thanks are welcome to Andreas Hamann from Alberta University for all support during the research and for the climate data models provided. The second affiliation of the author is Earthresearch Company, Department of Hydrogeology, Cluj-Napoca, Romania.

Table 3. Corine Land Cover classes and annual Kc calculated for present in Italy.

Corine Land Cover		Kc annual				
CLC code 2012	CLC Description	Kc	Ks	Ku	Kw	Kclc
111	Continous urban fabric	-	-	0.29	-	0.29
112	Discontinuous urban fabric	-	-	0.21	-	0.21
121	Industrial or commercial units	-	-	0.3	-	0.3
122	Road and rail networks and associated land	-	-	0.25	-	0.25
123	Port areas	-	-	0.39	-	0.39
124	Airports	-	-	0.3	-	0.3
131	Mineral extraction sites	-	-	0.26	-	0.26
132	Dump sites	-	-	0.26	-	0.26
133	Construction sites	-	-	0.26	-	0.26
141	Green urban areas	-	-	0.21	-	0.21
142	Sport and leisure facilities	-	-	0.21	-	0.21
211	Non-irrigated arable land	1.14	-	-	-	1.14
212	Permanently irrigated land	1.25	-	-	-	1.25
213	Rice fields	0.94	-	-	-	0.94
221	Vineyards	0.5	-	-	-	0.5
222	Fruit trees and berry plantations	0.68	-	-	-	0.68
223	Olive groves	0.66	-	-	-	0.66
231	Pastures	0.7	-	-	-	0.7
241	Annual crops associated with permanent crop	0.67	-	-	-	0.67
242	Complex cultivation patterns	1.16	-	-	-	1.16
243	Land principally occupied by agriculture, with significant areas of natural vegetation	0.92	-	-	-	0.92
244	Agro-forestry areas	0.92	-	-	-	0.92
311	Broad-leaved forest	1.42	-	-	-	1.42
312	Coniferous forest	1	-	-	-	1
313	Mixed forest	1.33	-	-	-	1.33
321	Natural grasslands	0.97	-	-	-	0.97
322	Moors and heathland	0.92	-	-	-	0.92
323	Sclerophyllous vegetation	0.62	-	-	-	0.62
324	Transitional woodland-shrub	0.83	-	-	-	0.83
331	Beaches, dunes, sands	-	0.23	-	-	0.23
332	Bare rocks	-	0.15	-	-	0.15
333	Sparsely vegetated areas	0.48	-	-	-	0.48
334	Burnt area	-	0.1	-	-	0.1
335	Glaciers and perpetual snow	-	-	-	0.5	0.51
411	Inland marshes	-	-	-	0.5	0.45
412	Peat bogs	-	-	-	0.4	0.37
421	Salt marshes	-	-	-	0.3	0.32
422	Salines	-	0.1	-	-	0.1
423	Intertidal flats	-	-	-	0.6	0.64
511	Water courses	-	-	-	0.6	0.63
512	Water bodies	-	-	-	0.6	0.64
521	Coastal lagoons	-	-	-	0.7	0.68
522	Estuaries	-	-	-	0.6	0.62
523	Sea and ocean	-	-	-	0.7	0.74

Table 4. Corine Land Cover classes and calculated annual Kc for future scenarios in Italy.

Corine Land Cover			Kc				
CLC code 2012	CLC projection code	CLC Description	Kc	Ks	Ku	Kw	Kclc
133	0	Built-up area	-	-	0.3	-	0.26
211	1	Arable land (non-irrigated)	1.1	-	-	-	1.14
231	2	Pasture	0.7	-	-	-	0.7
321and 324	3	Natural and semi-natural vegetation (including Natural grasslands, scrublands, regenerating forest below 2 m, and small forest patches within agricultural landscapes)	0.9	-	-	-	0.9
411	4	Inland wetlands	-	-	-	0.45	0.45
335	5	Glaciers and snow	-	-	-	0.51	0.51
212	6	Irrigated arable land	1.3	-	-	-	1.25
321	7	Recently abandoned arable land (i.e. "long fallow"; includes very extensive farmland not reported in agricultural statistics, herbaceous vegetation, grasses and shrubs below 30 cm)	1	-	-	-	0.97
241	8	Permanent crops	0.7	-	-	-	0.67
313	10	Forest	1.3	-	-	-	1.33
333	11	Sparsely vegetated areas	0.5	-	-	-	0.48
331	12	Beaches, dunes and sands	-	0.2	-	-	0.23
422	13	Salines	-	0.1	-	-	0.1
423 and 521	14	Water and coastal flats	-	-	-	0.66	0.66
322	15	Heathland and moorlands	0.9	-	-	-	0.92
231and 324	16	Recently abandoned pasture land (includes very extensive pasture land not reported in agricultural statistics, grasses and	0.8	-	-	-	0.76

REFERENCES

Adamo, F., De Capua, C., Filianoti, P., Lanzolla, A.M.L. & Morello, R. (2014) A coastal erosion model to predict shoreline changes. *Measurement*, 47, 734–740.

Allen, R.G., Pereira, L.S., Raes, D. & Smith, M. (1998) *Crop Evapotranspiration: Guidelines for Computing Crop Water Requirements.* FAO Irrigation and Drainage Paper 56. FAO: Rome, pp. 300.

Allen, R.G. (2000) Using the FAO-56 dual crop coefficient method over an irrigated region as part of an evapotranspiration intercomparison study. *Journal of Hydrology*, 229, 27–41.

Angelini, M.G., Costantino, D. & Di Nisio, A. (2017) *ASTER image for environmental monitoring: Change detection and thermal map*. IEEE International Instrumentation and Measurement Technology Conference, Proceedings, 7969745.

Brouyère, S., Carabin, G. & Dassargues, A. (2004) Climate change impacts on groundwater resources: modelled deficits in a chalky aquifer, Geer basin, Belgium. *Hydrogeology Journal*, 12, 123–134.

Campos, G.E.P., Moran, M.S., Huete, A., Zhang, Y., Bresloff, C., Huxman, T.E. et al. (2013) Ecosystem resilience despite large-scale altered hydroclimatic conditions. *Nature*, 494, 349–353.

Copernicus Land Monitoring Services. (2012) CORINE Land Cover of Europe. URL: http://land.copernicus.eu/ (accessed 21 July 2016).

European Environmental Agency. (2007) *Land-use scenarios for Europe: qualitative and quantitative analysis on a European scale*. ISSN 1725-2237. EEA Technical report No 9/2007.

Gowda, P.H., Chavez, J.L., Colaizzi, P.D., Evett, S.R., Howell, T.A. & Tolk, J.A. (2008) ET mapping for agricultural water management: present status and challenges. *Irrigation Science*, 26(3), 223–237.

Grimmond, C.S.B. & Oke, T.R. (1999) *Evapotranspiration rates in urban areas, Impacts of Urban Growth on SurfaceWater and Groundwater Quality*. Proceedings of IUGG 99 Symposium HSS. Birmingham, July 1999.

Hamann, A., Wang, T., Spittlehouse, D.L. & Murdock, T.Q. (2013) A comprehensive, high-resolution database of historical and projected climate surfaces for western North America. *Bulletin of the American Meteorological Society*, 94, 1307–1309.

Kottek, M., Grieser, J., Beck, C., Rudolf, B. & Rubel, F. (2006) World Map of the Köppen-Geiger climate classification updated. *Meteorologische Zeitschrift*, 15(3), 259–263.

Li, K.Y., Coe, M.T., Ramankutty, N. & De Jong, R. (2007) Modeling the hydrological impact of land-use change in West Africa. *Journal of Hydrology*, 337, 258–268.

Loàiciga, H.A., Maidment, D.R. & Valdes, J.B. (2000) Climate-change impacts in a regional karst aquifer, Texas, USA. *Journal of Hydrology*, 227, 173–194.

Nistor, M.M., Cheval, S., Gualtieri, A., Dumitrescu, A., Boţan, V.E., Berni, A., Hognogi, G., Irimuş, I.A. & Porumb-Ghiurco, C.G. (2017) Crop evapotranspiration assessment under climate change in the Pannonian basin during 1991-2050. *Meteorol. Appl.*, 24, 84–91.

Parmesan, C. & Yohe, G. (2003) A globally coherent fingerprint of climate change impacts across natural systems. *Nature*, 421(2), 37–42.

Prăvălie, R., Sîrodoev, I. & Peptenatu, D. (2014) Detecting climate change effects on forest ecosystems in Southwestern Romania using Landsat TM NDVI data. *Journal of Geographical Sciences*, 24, 815–832.

Rogan, J. & Chen, D.M. (2004) Remote sensing technology for mapping and monitoring land-cover and land-use change. *Progress in Planning*, 61(4), 301–325.

Rosenberry, D.O., Winter, T.C., Buso, D.C. & Likens, G.E. (2007) Comparison of 15 evaporation methods applied to a small mountain lake in the northeastern USA. *Journal of Hydrology*, 340, 149–166.

Schulp, C.J.E., Tieskens, K.F., Sturck, J., Fuchs, R., van der Zanden, E.H., Schrammeijer, E. & Verburg, P.H. (2015) *EU scale analysis of future cultural landscape dynamics*. Report no. 1, WP 5 Fine- and broad-scale modelling of future landscapes.

Thornthwaite, C.W. (1948) An approach toward a rational classification of climate. *Geogr. Rev.*, 38, 55–94.

Treitz, P. & Rogan, J. (2004) Remote sensing for mapping and monitoring land-cover and land-use change—an introduction. *Progress in Planning*, 61, 269–279.